Spinning and Properties of Poly(Ethylene Terephthalate)/ Organomontmorillonite Nanocomposite Fibers

Guo-Hu Guan,[1,2] Chun-Cheng Li,[1] Dong Zhang[1]

[1]*Key Laboratory of Engineering Plastics, Joint Laboratory of Polymer Science and Materials, Institute of Chemistry, the Chinese Academy of Sciences, Beijing 100080, China*
[2]*Graduate School of the Chinese Academy of Sciences, Beijing 100039, China*

Received 15 January 2004; accepted 11 September 2004
DOI 10.1002/app.21387
Published online in Wiley InterScience (www.interscience.wiley.com).

ABSTRACT: By *in situ* polycondensation, a intercalated poly(ethylene terephthalate)/organomontmorillonite nanocomposite was prepared after montmorillonite (MMT) had been treated with a water-soluble polymer. This nanocomposite was produced to fibers through melt spinning. The resulting nanocomposite fibers were characterized by X-ray diffraction (XRD), differential scanning calorimeter (DSC), and transmission electron microscopy (TEM). The interlayer distance of MMT dispersed in the nanocomposite fibers was further enlarged because of strong shear stress during processing of melt spinning. This was confirmed by XRD test and TEM images. DSC test results showed that incorporation of MMT accelerated the crystallization of poly(ethylene terephthalate) (PET), but the crystallinity of the drawn fibers just had a little increasing compared with that of neat PET drawn fibers. Also compared with pure PET drawn fibers, tensile strength at 5% elongation and thermal stability of the nanocomposite fibers were improved. © 2005 Wiley Periodicals, Inc. J Appl Polym Sci 95: 1443–1447, 2005

Key words: poly(ethylene terephthalate); nanocomposite; fiber; properties

INTRODUCTION

In recent years, polymer/layered silicate nanocomposites have been a research focus of scientists from all over the world because of its tremendously improved properties such as excellent mechanical properties, thermal stability, gas barrier, and fire retardence compared with conventional composites.[1–9] Montmorillonite (MMT) is the most widely used mica-type layered silicate, and it is composed of two silica tetrahedral sheets and a lumina octahedral sheet. Because of isomorphous substitution, which means an atom of lower positive valence replaces one of higher valence, negative charges are generated in these clay layers.[10] Exchangeable metal ions existing in the interlayer space neutralize those negative charges, distributing in the surface of layers. Polymer/layered silicate nanocomposites can be prepared by *in situ* polymerization,[6,9,11–14] melt blending,[2,15–17] or solution blending[18] after ion exchange of MMT with organic cations, which leads to expanding of interlayer distance and modifying of surface polarity of clay layers. Two kinds of nanocomposites, intercalated or exfoliated, will form according to the dispersion state of clay layers in polymer matrix. Usually an exfoliated nanocomposite has better properties than an intercalated one because of its better structure uniformity.

Poly(ethylene terephalate) (PET) is a widely used semicrystalline thermoplastic polyester with excellent properties such as very good barrier, crease resistance, solvent resistance, high melting point, resistance to fatigue, and high tenacity as either a film or a fiber. However, there is a continuing practical need to improve the performance properties of PET. Usually, copolymerization and blending with other polymers are effective ways in the chemical or physical modification of PET, and a series of new materials with better performance compared with PET was yielded in the last a few years.[19–22] Recently, in light of success in research of some polymer/clay nanocomposites, preparation of PET/clay nanocomposite has become another popular method to improve the performance of PET,[9,13,14,16,23,24] although molecular mass degradation and alkyl ammonium degradation during processing of some polymer/layered silicate nanocomposites have both been observed,[25–27] and those surfactants with higher thermal stability were widely used.[13,14,16,28–30] Despite the great effort in this area over the past a few years, challenges still remain to be solved to produce PET/layered silicate nanocomposite of exfoliated style, especially of commercial quality.

Up to now, only a few studies have been reported on the spinning of polymer/MMT nanocomposites.[31] Could the excellent mechanical and thermal proper-

Correspondence to: C.-C. Li (lizy@iccas.ac.cn).
Contract grant sponsor: National Basic Research Program: contract grant number: 2003CB615605.

ties of polymer/MMT nanocomposites be exhibited in their fibers? In this article, an intercalated PET/organo-MMT nanocomposite was prepared through *in situ* polycondensation, and then the acquired material was produced to fibers by melt spinning. The structure and properties of this material and its fibers were studied in detail.

EXPERIMENTAL

Materials

Sodium-MMT with a cation exchange capacity of 100 mequiv/100 g and a nominal particle size of 40 μm was obtained from Institute of Chemical Metallurgy, Chinese Academy of Sciences (China). Poly(vinylpyrrolidone) (PVP) was purchased from Beijing Chemical Reagents Company (China). Dimethyl terephthalate (DMT) was a commercial product from Mitsubishi Chemical Corp. (Japan). Zinc acetate and antimony trioxide of analytical purity were also purchased from Beijing Chemical Reagent Company (China) and used without further purification.

Preparation of organo-MMT

A suspension of 1 part of sodium-MMT by weight in 40 parts of distilled water by weight, in which 1 part of PVP by weight was dissolved, was stirred vigorously. The temperature was maintained at 90°C for 4 h. Then the precipitate was filtered and washed with distilled water three times. The acquired MMT was dried in a vacuum to a constant weight at 80°C and then ground into powder.

Synthesis of PET/organo-MMT nanocomposite

A given weight of organo-MMT powder was dispersed uniformly in 100 parts of DMT by weight, 72 parts of ethylene glycol by weight, and a zinc acetate catalyst. The mixture was heated to about 180°C, whereupon methanol was generated. After a theoretical amount of methanol was removed, an antimony trioxide catalyst was added to the reaction system and the pot temperature was increased to $\sim$ 280°C. At the same time, a vacuum was applied ($<$0.1 mmHg) to produce PET/organo-MMT nanocomposite. Pure PET was also synthesized in our lab with the same method but no organo-MMT powder was added.

Spinning

All the samples were dried in a vacuum oven at 130°C for at least 10 h before the spinning operation. Melt spinning was performed on a small-type spin apparatus with a spinning temperature of $\approx$ 285°C; the spinning speed was 500 m/min. Then, the acquired as-spun fibers of 50 filaments were drawn with a draw ratio of 4.98 under regular condition.

Measurements

Differential scanning calorimeter (DSC)

A Perkin–Elmer DSC-7 differential scanning calorimeter thermal analyzer was used for DSC analysis. Each sample of $\sim$ 8 mg was accurately weighed before being placed in DSC span. Under nitrogen atmosphere, it was heated from room temperature to 300°C with a heating rate of 20°C/min. The sample was kept for 10 min at this temperature to eliminate the heat history before cooling at 20°C/min.

Thermogravimetric analysis (TGA)

A Perkin–Elmer 7 Series thermal analysis system was used to perform thermogravimetric analysis. Samples were heated at 20°C/min from ambient temperature to 800°C in a nitrogen atmosphere. The standard uncertainty of decomposition temperature reported is $\pm$1°C.

X-ray diffraction (XRD)

In Saritzkey–Golay's mode, XRD was performed at room temperature by a Ragaku Model D/max-2B diffractometer at a generator voltage of 40 kV and a generator current of 100 mA. Testing data were collected from 1.5° to 40° at a scanning rate of 2°/min.

Transmission electron microscope (TEM)

The type of TEM used was JEOL-100CX and the acceleration voltage was 100 kV. All fiber samples were first put into epoxy capsules. Both these samples and those pellet samples were all microtomed by a diamond knife into 50- to 80-nm-thick slices.

Tensile properties

Tensile testing was carried out on a universal tester (Instron 1122) based on internationally agreed methods for testing polyester filament yarns (1983 edition) of BISFA. The length of samples was 500 mm, and the extension rate was 500 mm/min. The average values of 10 tests were reported.

Heat shrinkage

The heat shrinkage test was performed on a ventilated oven at the temperature of 177 $\pm$ 1°C based on ASTM D 4974-1993. The length of samples was 250 mm, and a strain of 0.5 $\pm$ 0.05 cN/tex was applied beforehand.

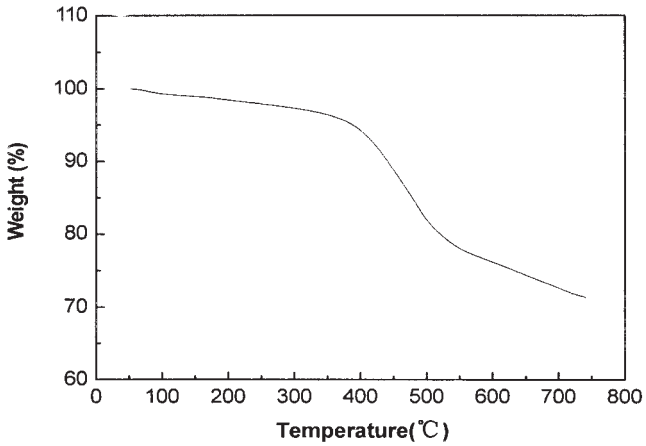

Figure 1 TGA curve of PVP-MMT measured under a nitrogen atmosphere.

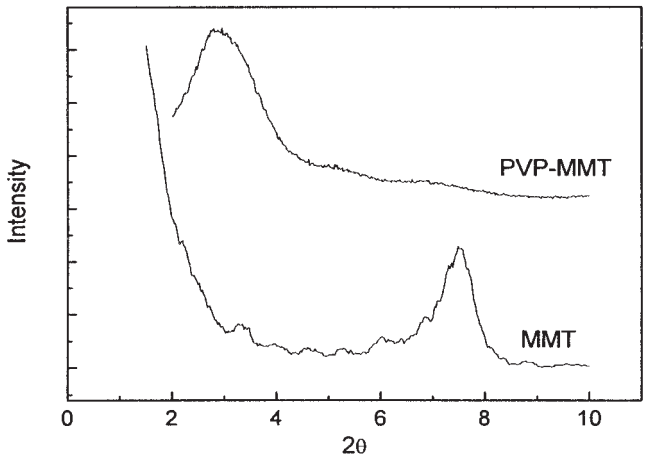

Figure 2 XRD patterns of MMT and PVP-MMT.

The test maintained 10 min every time, and the average values of 10 tests were reported.

RESULTS AND DISCUSSION

Pretreatment of MMT is of great importance for the reason that intercalation of macromolecules and polymerization precursors extremely depends on the expanding extent of interlayer distance, surface polarity of silicate layers, and compatibility of organic modifier with polymer matrix. In addition, thermal stability of organic modifier is also very important, especially for PET, because the synthesis and processing temperature of PET is so high (near 300°C) that some most widely used organic modifiers such as alkylammonium have decomposed below this temperature, which may cause some negative effects on products.

PVP is a water-soluble polymer and in its water solution PVP macromolecules will be absorbed on the surface of silicate layers. So, PVP can be used as surface modifier of clay. Figure 1 shows the TGA thermogram of MMT treated with PVP (PVP-MMT). Obviously, its thermal stability is quite excellent because the weight loss onset temperature of PVP-MMT is ~ 400°C. Most alkyl imidazolium and alkyl phosphonium treatments for MMT have on onset of thermal decomposition much lower than this, although they have better thermal stability compared with alkylammonium treatments.

XRD analysis was used to determine whether the layer distance of PVP-MMT had changed. Figure 2 shows the XRD patterns of PVP-MMT and untreated MMT. In the low-angle region of the data, the peak shifts from 7.2° of untreated MMT to 2.8° of PVP-MMT, which indicates an increasing of layer distance from ~ 1.2 to ~ 3.2 nm according to Bragg's equation. Increasing layer distance will weaken interaction between MMT layers and will facilitate the exfoliation of MMT layers during synthesis and processing.

The compatibility of organo-clay with matrix is also of great importance to form a uniform nanocomposite. We found that organic modifiers having a long alkyl group usually led to poor compatibility with PET matrix because of their very low polarity. Functionalized alkyls may help to enhance the combination strength between MMT layers and PET matrix by way of covalent bonds, but they do not get the interlayer gallery much more thermodynamically favorable for the penetration of PET precursors and macromolecules. In our research, PVP-MMT was used to prepare PET/organo-MMT nanocomposites by *in situ* polymerization with a MMT loading of 1.5 wt %, and there would be some difficulty in the processing of melt spinning if more MMT was incorporated. XRD data (see Fig. 3) show that there is still a very low peak at 2θ angle of 3.7°, which indicates a layer distance of 2.4 nm. PET is one of the most important polymers used for synthetic fibers, including tire fabrics. In our re-

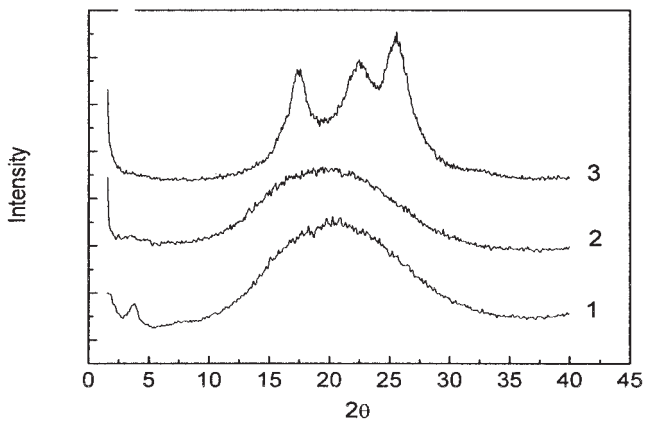

Figure 3 XRD curves of PET nanocomposite (1) pellet, (2) as-spun fibers, (3) drawn fibers.

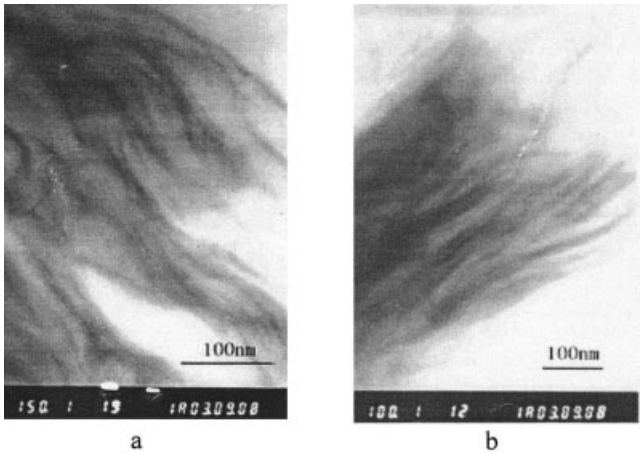

Figure 4 TEM images of (a) PET/organo-MMT nanocomposite and (b) its as-spun fibers.

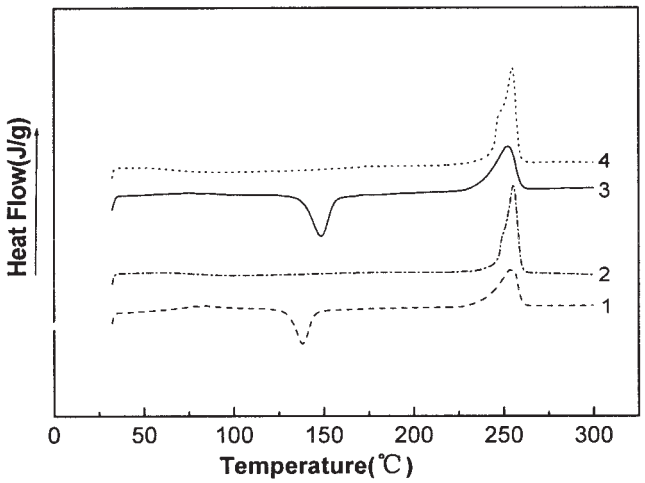

Figure 5 DSC thermograms of PET nanocomposite (1) as-spun fibers, (2) drawn fibers, and pure PET (3) as-spun fibers, (4) drawn fibers.

search, the PET/PVP-MMT nanocomposite was spun to fibers. Figure 3 also shows the XRD patterns of as-spun fibers and drawn fibers made of this material. There was no peak in low angle region for both these two fibers. It means that MMT layers have been exfoliated by strong shear stress during melt spinning.

Figure 4(a) is the TEM image of this nanocomposite. MMT layers still show a regular face-to-face style with expanded layer distance. Both XRD data and TEM image indicate a nice dispersion of organo-MMT in PET matrix, but they still lead to the conclusion that *in situ* polycondensation conditions are not fully optimized for preparing of completely exfoliated PET/organo-MMT nanocomposite.

Figure 4(b) is the TEM image of nanocomposite as-spun fibers. Compared with Figure 4(a), the interlayer space of MMT in as-spun fibers has been further expanded and even resulted in the arising of some single layers. This also proved that the strong shear stress during melt spinning induced the exfoliation of MMT.

So, those organo-MMT layers cannot be exfoliated during *in situ* polycondensation, but their interaction was weakened by intercalation of macromolecules. During melt spinning, further intercalation or even exfoliation can be realized because of strong shear action.

A DSC test was used to analyzes the thermal properties and crystallinity of these fibers. Figure 5 shows the thermograms of the as-spun and drawn fibers made of pure PET and PET nanocomposite. The cold crystallization temperature of the nanocomposite as-spun fibers was obviously lowered ≈ 10°C, and this is the result of heterogeneous nucleation of MMT layers, which leads to an acceleration of crystallization. Figure 5 also shows the thermograms of drawn fibers made of PET and PET/organo-MMT nanocomposite. The two kinds of fibers have crystallized to a significant degree during the processing of drawing, so their cold crystallization exothermal peaks cannot be observed. Besides, the XRD patterns also show a characteristic peak of PET crystal (see Fig. 3). According to the literature,[32–34] the DSC crystallinity (β_c) of these drawn fibers can be obtained from their DSC data. The crystallinity of nanocomposite drawn fibers was about 42.1%, just three points over that of neat PET drawn fibers. Obviously, incorporation of organo-MMT cannot have the crystallinity of drawn fibers remarkably increased, although it can accelerate the crystallization of PET nanocomposite.

The properties of PET and PET/MMT nanocomposite drawn fibers are listed in Table I. According to the data shown in Table I, incorporation of MMT has some advantageous effects on fibers; the heat shrinkage of PET/MMT nanocomposite drawn fibers was lowered, and the tensile strength at 5% elongation of PET/MMT nanocomposite drawn fibers was improved. The reason may be that the MMT layer dispersed uniformly in PET matrix restricted the movement of PET macromolecules. The results above mean

TABLE I
Properties of PET and PET/MMT Nanocomposites Drawn Fibers

Sample	PET drawn fibers	PET nanocomposite drawn fibers
Stretch ratio	4.98	4.98
Linear density (dtex)	126	121
Tenacity (cN/dtex)	5.30	5.08
Tensile strength at 5% elongation (cN/dtex)	3.04	3.15
Strain (%)	13.7	11.1
Heat shrinkage (%, 177°C, 10 min)	4.4	3.9

PET/MMT nanocomposite, drawn fibers have higher modulus and thermal stability than PET drawn fibers; this is especially important in the rubber tire industry, where PET fibers are used as tire fabrics.

Although incorporation of layered silicate can improve the strength of PET/layered silicate nanocomposite, Table I shows that the tenacity of PET/MMT nanocomposite drawn fibers had a slight decrease in comparison with that of pure PET draw fibers. Some other researchers also observed similar phenomenon when studying other polymer hybrid fibers.[31] The reason seems to be that imperfect bonding and debonding occurs at interface, and an imperfect incursion/matrix interface cannot sustain the large interfacial shear stress that develops as a result of an applied strain. This subject needs further research.

CONCLUSION

An intercalated PET/organo-MMT nanocomposite was prepared by *in situ* polycondensation. After melt spinning, the exfoliation of MMT layers was realized because of strong shear stress during the processing. Although incorporation of MMT can accelerate the crystallization of PET, it only had an unapparent effect on crystallinity of nanocomposite-drawn fibers. In addition, the tensile strength at 5% elongation and thermal stability of the fibers made of this nanocomposite was improved compared with those of pure PET fibers.

This work was supported by the National Basic Research Program of China (2003CB615605).

References

1. Yano, K.; Usuki, A.; Okada, A.; Kurauchi, T.; Kamigaito, O. J Polym Sci, Polym Chem Ed 1993, 31, 2493.
2. Giannelis, E. P. Adv Mater 1996, 8, 29.
3. Messersmith, P. B.; Giannelis, E. P. Chem Mater 1994, 6, 1719.
4. Hasegawa, N.; Okamoto, H.; Kato, M.; Usuki, A. J Appl Polym Sci 2000, 78, 1918.
5. Kawasumi, M.; Hasegawa, N.; Kato, M.; Usuki, A.; Okada, A. Macromolecules 1997, 30, 6333.
6. Usuki, A.; Kato, M.; Okada, A.; Kurauchi, T. J Appl Polym Sci 1997, 63, 137.
7. Kato, M.; Usuki, A.; Okada, A. J Appl Polym Sci 1997, 66, 1781.
8. Hasegawa, N.; Kawasumi, M.; Kato, M.; Usuki, A.; Okada, A. J Appl Polym Sci 1998, 67, 87.
9. Zhang, G. Z.; Shichi, T.; Takagi, K. Mater Lett 2003, 57, 1858.
10. Olphen, H. van An Introduction to Clay Colloid Chemistry; John Wiley & Sons: New York, 1977.
11. Usuki, A.; Kojima, Y.; Kawasumi, M.; Okada, A.; Fukushima, Y.; Kurauchi, T.; Kamigaito, O. J Mater Res 1993, 8, 1179.
12. Lan, T.; Pinnavaia, T. J. Chem Mater 1994, 6, 2216.
13. Imai, Y.; Nishimura, S.; Abe, E.; Tateyama, H.; Abiko, A.; Yamaguchi, A.; Aoyama, T.; Taguchi, H. Chem Mater 2002, 14, 477.
14. Imai, Y.; Inukai, Y.; Tateyama, H. Polym J 2003, 3, 230.
15. Liu, X. H.; Wu, Q. J. Polymer 2001, 42, 10013.
16. Davis, C. H.; Mathias, L. J.; Gilman, J. W.; Schiraldi, D. A.; Shields, J. R.; Trulove, P.; Sutto, T. E.; DeLong, H. C. J Polym Sci, Part B: Polym Phys 2002, 40, 2661.
17. Wan, C. Y.; Qiao, X. Y.; Zhang, Y.; Zhang, Y. X. Polym Testing 2003, 22, 453.
18. Jeon, H. G.; Jung, H. T.; Lee, S. D.; Hudson, S. Polym Bull 1998, 41, 107.
19. Xiao, J.; Wan, X. H.; Zhang, D.; Zhang, H. L.; Zhou, Q. F.; Turner, S. R. J Polym Sci, Part A: Polym Chem 2002, 40, 852.
20. Kint, D. P. R.; Alla, A.; Deloret, E.; Campos, J. L.; Guerra, S. M. Polymer 2003, 44, 1321.
21. Wu, G.; Cuculo, J. A. Polymer 1999, 40, 1011.
22. Ihm, D. W.; Park, S. Y.; Chang, C. G.; Kim, Y. S.; Lee, H. K. J Polym Sci, Part A: Polym Chem 1996, 34, 2841.
23. Zhang, G. Z.; Shichi, T.; Tong, Z. W.; Takagi, K. Chem Lett 2002, 3, 410.
24. Barber, G. D.; Moore, R. B. Abstr Pap Am Chem S 219: 131-PMSE, Part 2, Mar 26, 2000.
25. Gilman, J. W.; Jackson, C. L.; Morgan, A. B.; Harris, H. A.; Manias, E.; Giannelis, E. P.; Wuthenow, M.; Hilton, P.; Philips, S. H. Chem Mater 2000, 12, 1866.
26. VanderHart, D. L.; Asano, A.; Gilman, J. W. Chem Mater 2001, 13, 3796.
27. Davis, R. D.; Gilman, J. W.; VanderHart, D. L. Polym Degrad Stab 2003, 79, 111.
28. Gilman, J. W.; Awad, W. H.; Davis, R. D.; Shields, J. R.; Kashiwagi, T.; VanderHart, D. L.; Harris, R. H., Jr.; Davis, C. H.; Morgan, A. B.; Sutto, T. E.; Callahan, J.; Trulove, P. C.; DeLong, H. Chem Mater 2002, 14, 3766.
29. Zhu, J.; Morgan, A. B.; Lamelas, F. J.; Wilkie, C. A. Chem Mater 2001, 13, 3774.
30. Liang, Z. M.; Yin, J.; Xu, H. J. Polymer 2003, 44, 1391.
31. Chang, J. H.; An, Y. U.; Kim, S. J.; Im, S. Polymer 2003, 44, 5655.
32. Gupta, V. B.; Mondal, S. A.; Bhuvanesh, Y. C. J Appl Polym Sci 1997, 65, 1773.
33. Kong, Y.; Hay, J. N. Polymer 2002, 43, 3873.
34. Kong, Y.; Hay, J. N. Eur Polym J 2003, 39, 1721.